Nordic Hydrology, 31 (4/5), 2000, 301-316

Simulation of Snowmelt in a Subarctic Spruce Woodland: Scale Considerations

Paper presented at the 12th Northern Res. Basins/Workshop
(Reykjavik, Iceland – Aug.23rd -27th 1999)

Ming-ko Woo and Mark A. Giesbrecht
School of Geography and Geology, McMaster University
Hamilton, Ontario, Canada L8S 4K1

Subarctic woodlands comprise stands of spruce trees with varying degrees of openness, giving rise to large contrasts in melt rates within the forest. The spatial variability of the changing snow depth during a melt season was investigated at three scales (2, 4 and 16 m), using an example from a site in Yukon, Canada, where the computation of snowmelt takes into account the differential rates within the woodland. During the melt period, the mean daily snow depth decreases but the variability increases as continued ablation leads to greater unevenness of the snow cover. At the three scales of representation, increasing the grid size results in a reduction in the standard deviation and the skewness of depth distribution. The blurring of snow cover pattern at the larger scales is due to a loss in information, considered as the absolute value of the difference in snow depth calculated at two scales for the same location. This loss increases as the snow depth becomes more variable during the melt season. Knowledge of the scale-induced information loss is relevant to the modelling of snowmelt that exhibits large spatial variations.

Introduction

Snowmelt in a subarctic woodland environment is a major hydrological event, driven by climatological conditions but modified by the presence of a tree cover of various stand densities. Melt runoff often triggers the annual floods, and a knowledge of timing and intensity of melt in northern forests has environmental significance and

practical applications. Depending on the purpose of application, snowmelt is studied at different scales (Woo 1998). However, point melt values have often been substituted for melt over an area without the consideration of their representativeness. At the other extreme, mean melt data for large grid cells from land surface schemes cannot be downscaled easily for hydrological investigations at basin or slope scales because of insufficient local detail. The question of resolution requires attention in the modelling of spatial snowmelt.

The scale problem[1] in snow investigations has been discussed by various authors (Blöschl *et al.* 1991a; Blöschl *et al.* 1991b; Davis1995; Garen and Marks 1996). There remains the need for empirical studies to compare the same set of material presented at different scales to identify the information that is preserved or lost due to snow data aggregation or disaggregation. In a simple conceptualization, a linear model describes a possible formulation of snow depth information to comprise two components

$$d' = \mu + \lambda \quad (1)$$

where d' is snow depth represented at a particular scale, μ is the mean depth over an area and γ is variation manifested at this scale of study within the domain of interest. Representing the snow data at a larger scale (d''), the mean over the area remains the same but some of the local variation is blurred, causing a loss of information $\Delta\rho$, or

$$d'' = \mu + (\lambda - \Delta\rho) \quad (2)$$

This conceptual model offers a tentative framework to appraise the spatial information represented at various scales.

Snowmelt in forests has been investigated at various levels of generalization (Buttle and McDonnell1987; Hardy *et al.* 1997, 1998; Hendrie and Price 1978). Snow depth depletion in a subarctic woodland, examined at the scales of 2, 4 and 16 m, is the subject of the present study. An energy balance model simulates snowmelt and a Geographic Information System (GIS) allows detailed representation of the spatial snow cover pattern during melt. Snow depths are mapped at the three scales and summarized by descriptive statistics. The purpose of the study is to compare the characteristics of snow depth information presented at several scales of investigation, from the pre-melt condition, through the main melt period until the snow begins to fragment. The results are relevant to the issue of scale in the modelling of a melting snow cover.

---

[1] Scale is here defined as the representation of a phenomenon at a particular ratio in the spatial dimension or at a specific interval in the time domain.

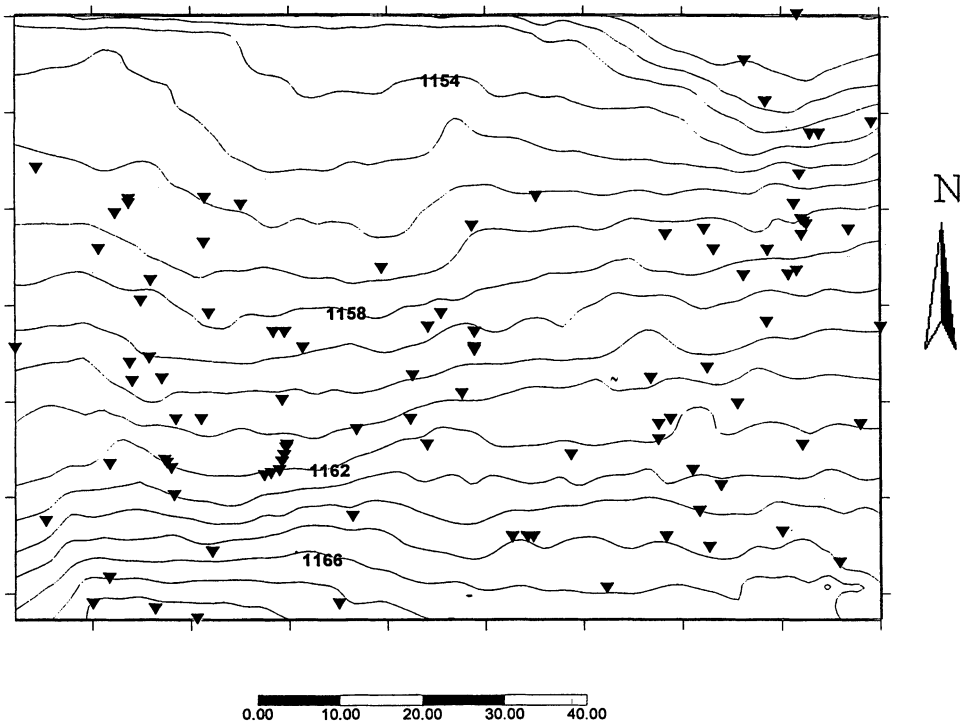

Fig. 1. Topography of the study slope in central Wolf Creek basin, Yukon. Triangular symbols indicate spruce trees on the slope, with the overall distribution pattern being typical of an open woodland in a subarctic setting.

Methods

Field work was carried out on a north-facing slope in central Wolf Creek basin near Whitehorse, Yukon, Canada (60.5°N, 135.1°W, elevation 1,150 m, mean gradient 10°) to derive empirical equations, obtain coefficients and to make meteorological measurements for snowmelt calculation. The slope has a subarctic open woodland with stands of white spruce and shrubs of alder and willow. A meteorological tower was erected in a woodland opening to measure solar radiation, air temperature, wind speed and relative humidity during the snowmelt period of April 10 to May 15 (or Julian days 110-135) 1997. Auxiliary measurements of the same variables were made at several points within and outside a spruce tree canopy to derive relationships for extrapolating the tower-site data to various zones in the woodland.

Subarctic woodlands have tree densities that range from sparse to close stands. The study plot measures 64x80 m^2 and contains 98 trees with trunk diameters greater than 0.1 m (Fig. 1). The location, heights, the trunk and canopy radii of all

the trees on the experimental slope were mapped. The presence of trees usually punctuates an otherwise relatively uniform snow surface due to the formation of tree wells around individual trees (Woo and Steer 1986). Sturm (1992) described the tree well profiles with the following relationship

$$d = d_0 - d_0 (a_1 - 1) \exp\left[-\left(\frac{D}{a_2}\right)^2\right] \quad (3)$$

where d is snow depth at a distance D from the tree trunk, d_0 is mean snow depth in the opening, a_1 and a_2 are empirical coefficients. An end-of-winter survey of snow profiles around the spruce trees yielded d_0 = 0.70 m, while a_1 and a_2 vary with tree trunk radius (r): for r<0.35 m, a_1=0.8, a_2=1; 0.35<r<0.5, a_1=0,7, a_2=1.5; r>0.5, a_1=0.6, a_2=2. An initial snow cover in the woodland was approximated by simulating a relatively even snow surface with hollows around the trees calculated using Eq.(3).

For snowmelt computation, the woodland is distinguished into four snowmelt categories: 1) tree trunk, 2) tree canopy, 3) open area in the sun and 4) in the tree shadow. Tree trunks and canopies cover only 2.7 per cent of the study area while the per centages of tree shadows and sunny areas vary during the day. Each tree is represented as a cylinder that casts its shadow on the snow. For the daylight hours (0600 to 1900 Pacific Standard Time), the shadow zones are generated hourly using the HILLSHADE command in Arc/INFO. Fig.2 provides examples of the shadow patterns produced during different times of a day. The resultant distributions of canopy, tree trunks, sunny and shady zones on the experimental slope are overlain by grid templates of 2x2, 4x4 and 16x16 m^2 dimensions to extract the fractional coverages of the four categories within each grid cell. Table 1 summarizes the fraction of open area in each grid cell at the three scales of investigation. The average slope orientation and gradient are extracted from the topographic map for the cells of the three sizes using the re-sampling method provided in Arc/INFO.

Table 1 – Number of grid cells with various fractions of open areas

Fraction of open areas in each cell	2-m scale cells	4-m scale cells	16 m scale cells
≤0.1	4	2	0
0.11-0.20	1	0	0
0.21-0.30	4	0	0
0.31-0.40	2	0	0
0.41-0.50	4	0	0
0.51-0.60	8	0	0
0.61-0.70	13	3	0
0.71-0.80	13	5	0
0.81-0.90	29	14	0
0.91-1.00	1202	296	20

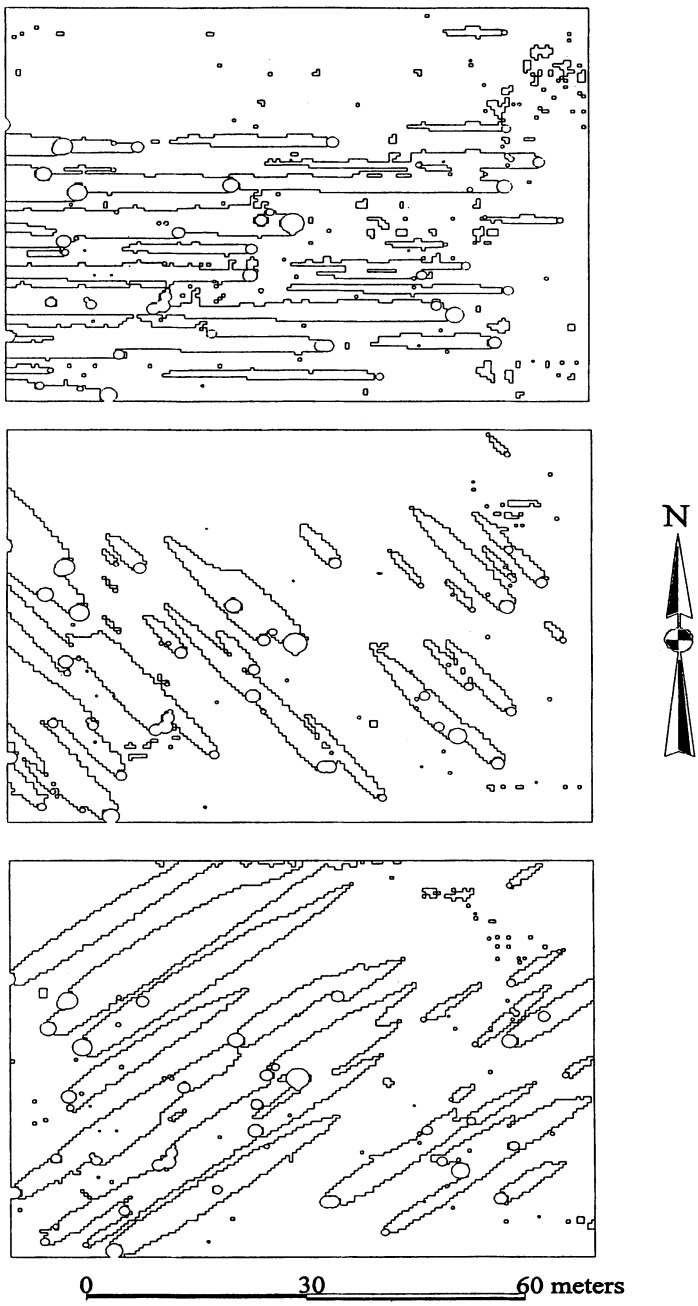

Fig. 2. Examples showing the shifting pattern of tree shadows cast by the spruce trees in the subarctic open woodland during mid-April at 0700 Pacific Standard Time (top), 1000 PST (middle) and at 1500 PST (bottom).

Snowmelt is calculated using the energy balance approach, using incoming solar radiation, air temperature, relative humidity and wind speed measured at an opening site as inputs. Details of the computational methods and the field measurements made during the melt season are given in Woo and Giesbrecht (2000) and only brief descriptions are presented below. Rain on snowmelt is not considered as there was no rain event during the study period. For radiation melt, the shadow zone in the opening and beneath the tree canopy receives diffuse radiation; but both direct and diffuse short-wave radiation are received in the sunny zone in the opening. Short-wave radiation ($K\downarrow$) is adjusted for the mean slope gradient of individual grid cell by

$$K\downarrow(\text{slope}) = K\downarrow(\text{horizontal})\cos\theta \tag{4}$$

where θ is the angle of incidence between the sun and the normal to the slope.

Short-wave radiation receipt is $(1-\alpha)K\downarrow$, with α being the snow albedo which declines during the melt season, following the approximation given by Woo and Dubreuil (1985)

$$\alpha(\tau) = \alpha_o - \frac{(\alpha_o - \alpha_g)}{\exp(b_1 + b_2\tau) + 1} \tag{5}$$

where $\alpha_o = 0.85$ is the albedo on day $\tau=0$ (day before melting began) and $\alpha_g = 0.2$ is albedo of bare ground; b_1 and b_2 are empirically found to be 3.24 and 0.19 respectively. Long-wave radiation (L) is computed by

$$L = \varepsilon\sigma T^4 \tag{6}$$

where σ is the Stefan-Boltzmann constant. ε is the emissivity, being 0.95 for the snow and for the canopy. For open areas, it is replaced by a coefficient of 0.7 (Davies and Idso 1979) which is an approximation to the emissivity from the sky (ε_a) obtained by Idso and Jackson (1969) as a function of air temperature (T_a)

$$\varepsilon_a = 1 - 0.261\exp(-7.77\times10^{-4}T_a^2) \tag{7}$$

T is temperature, considered to be 0°C for the ripened snow, and is taken as the air temperature for the open area. Air temperature beneath the canopy is found to be 1°C lower than the air temperature in the opening, as is suggested by the measurements obtained during the field season (Fig. 3).

The bulk transfer method (Price and Dunne 1976) is used to compute the sensible and latent heat fluxes. For the zone under the canopy, wind speed is modified according to an empirical relationship derived from field data (Fig. 3)

$$u_c = ku_z \tag{8}$$

with u_c and u_z being the wind speed under the tree and in the open area, and

$$k = 0.92\{1-\exp[-(1.2u_z - u_o)]\} \text{ for } u_z > u_o \qquad k = 0 \text{ when } u_z \leq u_o \tag{9}$$

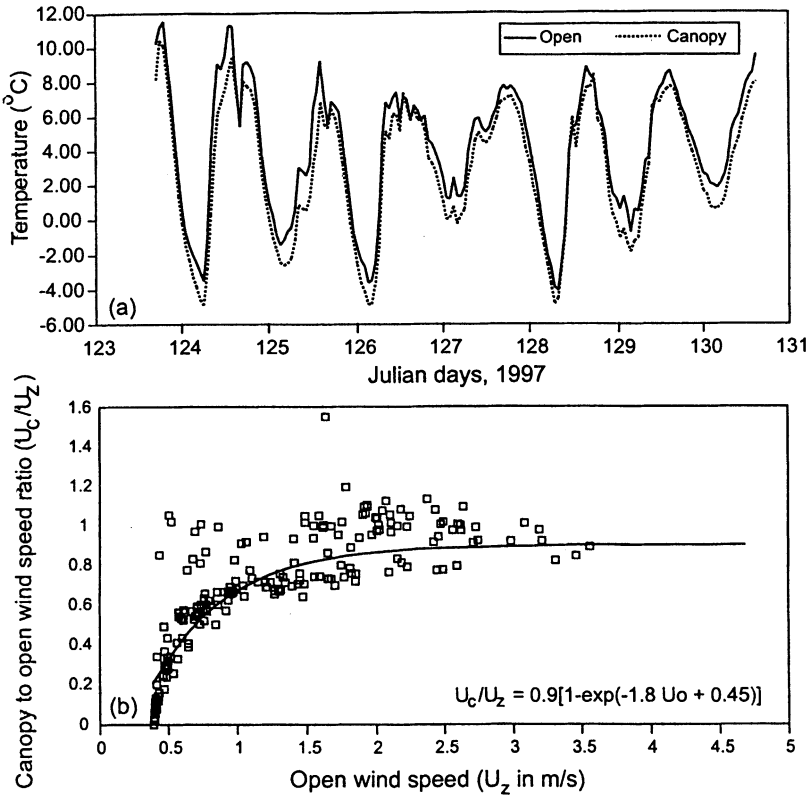

Fig. 3. (Top) hourly air temperature in the opening compared with temperature below a spruce tree canopy, indicating that the canopy temperature averages 1°C cooler than the opening. (Bottom) ratio of wind speed underneath a tree canopy to opening wind speed, expressed as an empirical function of wind speed in the open, based on field data of 1997.

where u_o=0.45 m/s is the open-site wind speed below which the speed is zero under the tree.

Snowmelt has to be calculated at hourly intervals in order to take account of the shifting shadow patterns. The hourly melt rates (in water equivalent units) are computed for the four melt categories, with the tree trunk category being zero. The average melt rate for each grid cell M is obtained by

$$M = \sum_{k=1}^{4} f_k m_k \qquad (10)$$

where m_k and f_k are the melt and fractional area for category k. For the present application, only daily snowmelt is considered so that the hourly melt rates are

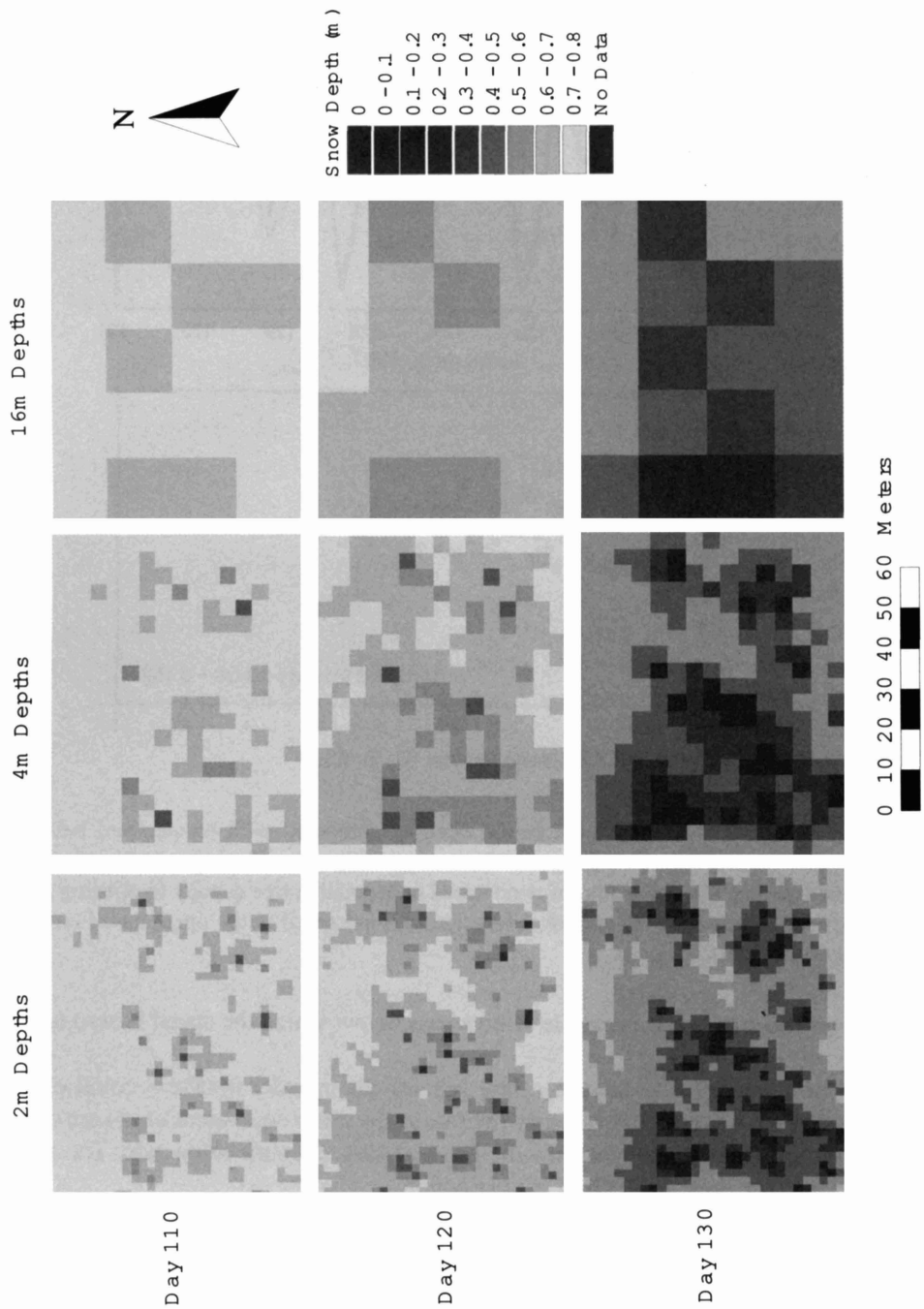

Fig. 4. Pattern of snow depth distribution in the woodland during the melt season of 1997, presented at three scales.

summed for the day and then converted to snow depth using snow densities which, according to field measurement, had an initial value of 300 kg/m^3. By the end of the study period, snow density reached 400-450 km/m^3 so that for the model, a daily density increase of 5 kg/m^3 was adopted. The daily melt depths for the various grid cells are used to update the snow depth maps (Giesbrecht and Woo 2000).

Snow Depth Patterns

The snow distribution patterns are mapped on the scales of 2, 4 and 16 m (Fig. 4). The influence of scale on snow depth representation is transmitted through the fractional areas of opening, canopy and tree trunk in each grid cell (*i.e.* m_k in Eq. (10)) do not change from one scale to the other. This differs from other approaches (*e.g.* Cline *et al.* 1998) which re-calculate the melt rates for all cells after the resolution is degraded to progressively larger scales.

At 2 m scale, the effects of individual trees on snow distribution and melt patterns can be discerned. Snow depth plotted at ten-day intervals indicates that the zones close to the tree exhibit the largest melt due to enhanced long wave radiation from the canopy. The western sector experiences greater melt, particularly in the first part of the melt season, because of the dense tree clusters. Later on, snowmelt accelerates in the open area as radiation intensifies and snow depth decreases more rapidly in the eastern sector. The northeastern corner of the slope with predominating small trees and in a topographical hollow retains deep snow throughout the melt period. One feature is the development of banded snow depth structure in the northwest, caused by the hourly time step of the model which gives rise to striped shadow zones with reduced snowmelt. This artifact of the model can be overcome by using shorter time intervals to calculate melt.

Computed snow depths at the 4 m scale indicate a general pattern of snow depth development similar to those revealed at the 2 m scale (Fig. 4). There is strong evidence of melt enhancement by the clusters of trees in the west, and deeper snow in the northeast. The snow distribution pattern is much simplified at the 16 m scale (Fig. 4). During the early stages of melt, localized melt around the trees disappears and only one cell in the northwestern section of the slope exhibits greater melt. Nevertheless, the enhanced melt effect of tree clusters remains and snow depth distribution still reflects this influence. The temporal banding effect at the northwestern corner seen at the 2 m and 4 m scales is eliminated as spatial averaging erases this local variability.

Statistical Characteristics of Snow Depth

The frequency distributions of snow depth are obtained from daily data generated at the 2 m scale (Fig. 5) to illustrate the changing statistical characteristics of the woodland snow cover during the melt period. The initial snow depth for the study site is

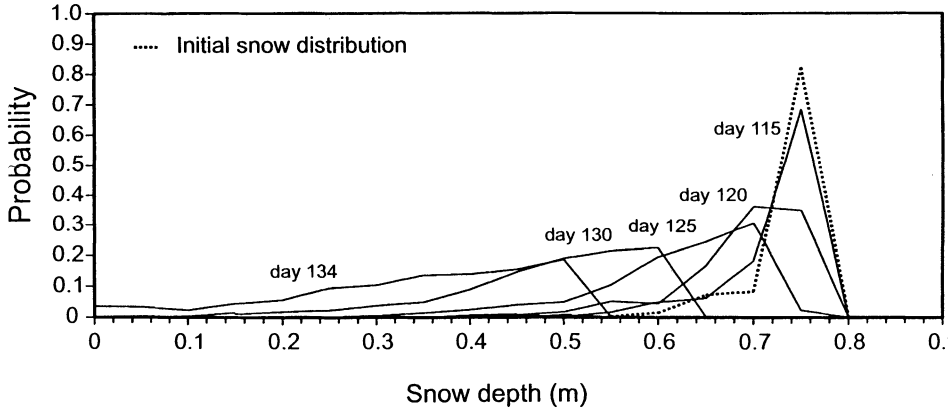

Fig. 5. Changing frequency distributions of snow depth in 2 m grid cells during the snowmelt season of 1997, indicating decreasing mean snow depth, increasing variability and lessening skewness as the snow melts in the open woodland.

relatively uniform except for the zones surrounding individual trees and this accounts for the high frequency of 0.75 m depths. Only cells containing tree wells produce lower snow depths (see Eq.(3)) so that the overall frequency distribution is highly skewed but with low variations in depth. As the melt season advances, mean snow depth decreases as does the skewness, but the variability increases. These features show that the snow depth becomes more uneven as the snow cover undergoes differential ablation.

The first three moments of snow distribution (the mean, standard deviation and skewness) are extracted for each day for comparison (Fig. 6). Initial snow depth obtained from the grid cells of the three scale averages 0.73 m. At the end of the study period, mean snow depths drops to 0.32 m. The standard deviations increase with time as the snow depth becomes more uneven and this tendency occurs at all scales, reaching 10-30 per cent of the mean snow depths at the end of the study period (Fig. 6). Such an increase is less for the 16-m scale due to the smoothing effect of its larger grid cells. This is consistent with other studies *(e.g.* Blöschl 1999) that the variability decreases if the cell values are aggregated into fewer units within the same region.

The averaging effect of large grid cells hides such detail as the occurrence of bare patches. At the end of the study period (day 134), 45 of the 1280 cells at the 2x2 m^2 scale have no snow, compared with only four of the 320 cells at the 4x4 m^2 scale and none of the 20 cells at the 16x16 m^2 scale. Thus, by averaging over a large grid-area, a cell is seldom completely bare even at the end of the main melt period.

Before melting begins, the relatively uniform snow surface is disrupted by individual trees and their snow wells and this gives rise to a strong negative skewness in snow depth distribution (Fig. 6). Skewness is not calculated for the 16 m grids be-

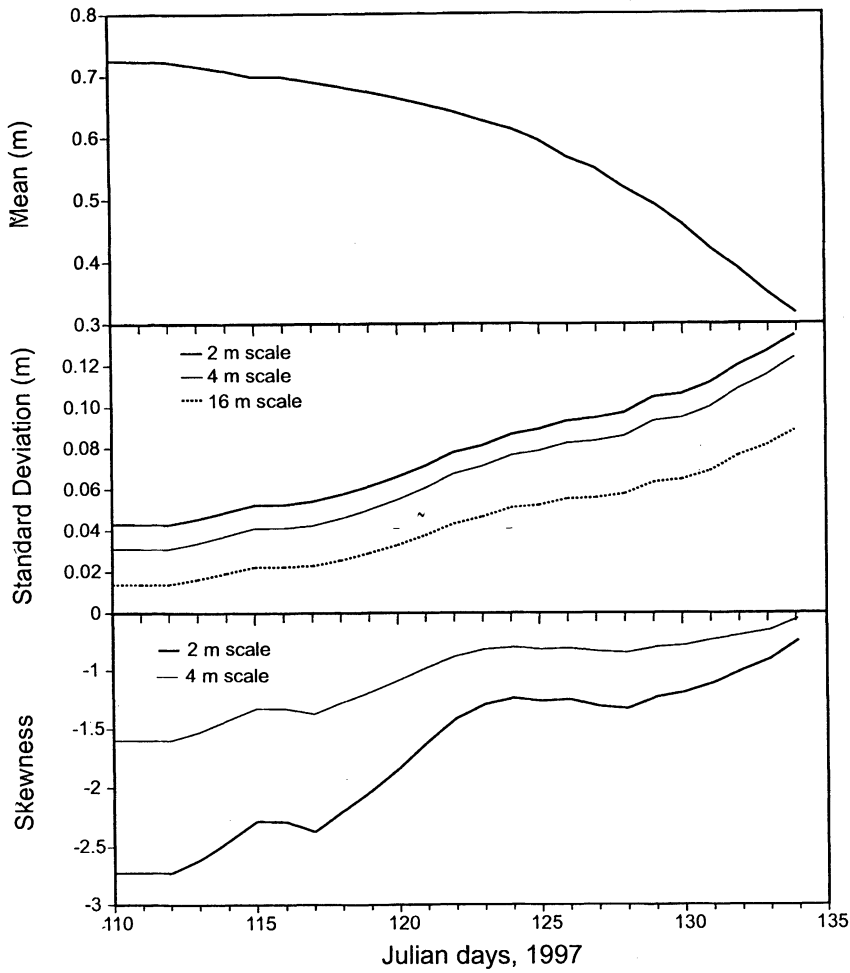

Fig. 6. Daily values of mean, standard deviation and skewness for snow depth in grid cells of various scales.

cause of limited samples (20 cells). During the melt season, skewness diminishes as spatially uneven melt rates break up the dominance of the pre-melt deep snow values and render the snow depth to be increasingly variable among grid cells.

Information Loss at Larger Scales

As shown by Fig. 4, snow depth variation around individual trees revealed at the 2 m scale is averaged out at the 4 m scale, and the tree cluster effects on snow depth exhibited at the 4 m scale becomes indistinct at the 16 m scale. Such loss of information due to upscaling is the physical manifestation of $\Delta\rho$ in Eq. (2). Further interpre-

tation of $\Delta\rho$ may be as follows. Consider a case where the scale is doubled (*i.e.* cell area is increased four times), snow depth at each large cell i is the mean of four adjacent cells of the smaller scale

$$d''_i = \sum_{j=1}^{4} \frac{d'_{ij}}{4} \tag{11}$$

The loss of information in terms of each cell of the finer scale is

$$\Delta d'_{ij} = |d'_{ij} - d''_i| = |d'_{ij} - \sum_{j=1}^{4} \frac{d'_{ij}}{4}| \tag{12}$$

Absolute values are used because regardless of the sign, the differences are a loss of information. Here, $\Delta d'_{ij}$ is an expression of $\Delta\rho$ in Eq.(2) . For cell i , the loss of information is the sum of the losses at the four small j-cells

$$\Delta d''_i = \sum_{j=1}^{4} \Delta d'_{ij} = \sum_{j=1}^{4} |d'_{ij} - \sum_{j=1}^{4} \frac{d'_{ij}}{4}| \tag{13}$$

Since absolute values are considered, total loss of information over an area depends on the variability of snow depth within cell i , and not on the mean depth of the cell. Hence, where the snow is uneven, upscaling suffers a greater loss of information than where the snow is uniform.

Calculation of the information loss at each grid cell requires matching the snow depth given at different scales for the same location. Thus, to compare the 2 and 4 m scales, a 4x4 m^2 cell is first divided into four sub-cells, each with an area of 2x2 m^2 and bearing the same snow depth. Depth in each sub-cell is compared with the snow depth in the 2 m cell at the equivalent location.

Fig. 7 shows the distribution of snow depth differences, or information loss Δd, between 2 and 4 m scales. At the initial period, snow depth is relatively even except around tree stands and most of the depth differences are around 0.05 m, with a few differences exceeding 0.1 m. As melt continues, the distribution becomes less peaked and more large values appear. This corresponds with the latter part of the melt period when differential melt in the woodland produces a cumulative effect to cause increasingly uneven snow depths. Similar changes are found in the distribution of Δd between the 4 and 16 m scales, though the distributions are less peaked than the Δd of 2 and 4 m scales for the corresponding periods. Comparison of the two sets of distributions indicates that between the 4 and 16 m scales, more areas in the woodland have larger Δd than between 2 and 4 m scales. Towards the end of the melt season, some cells show large differences (*e.g.* up to 0.5 m snow depth between the 4 and 16 m scale representations). This is due to the emergence of bare spots which are too small to affect the large-scale grids but which are reflected in the grid cells of the smaller scales.

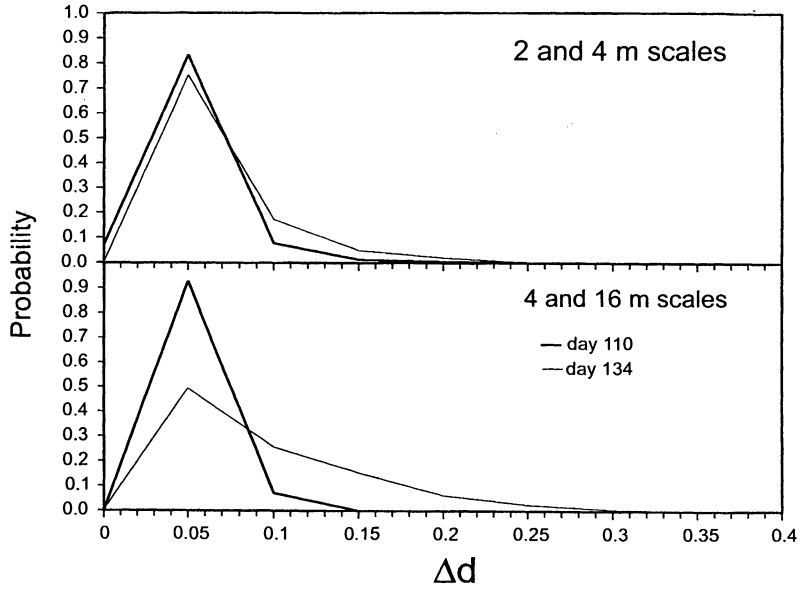

Fig. 7. Comparison of distribution functions of Δd (difference in snow depth at two scales) for the first and last days of the study.

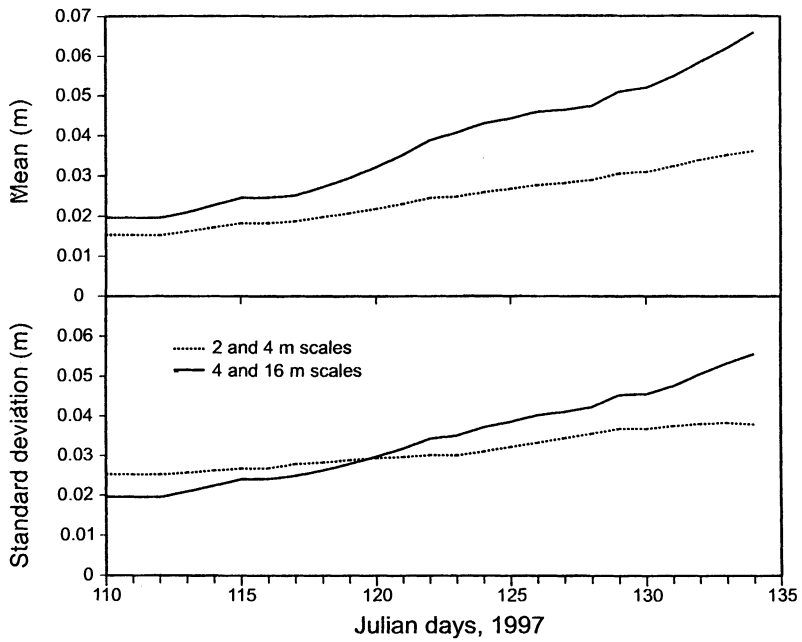

Fig. 8. Difference in snow depth (Δd) between 2 and 4 m scales, and 4 and 16 m scales: (top) mean and (bottom) standard deviation plotted against time of the snowmelt season.

Fig. 8 shows the means and standard deviations of Δd (as computed using Eq. (12)) between 2 and 4 m scales, and between 4 and 16 m scales. As expected from Eq.(13), increasing unevenness of the snow cover during the melt season causes mean Δd to increase. The standard deviation of Δd also rises as snowmelt progresses and this is attributed to the development of local variations in snow depth due to differential melt in different parts of the open woodland. The local variations are not captured at the larger scales and the loss of information becomes more irregular across the study area. Both the means and the standard deviations of Δd increase more rapidly for the 4-16 m scales than for the 2-4 m scales. The increasing mean values of Δd as melting advances suggests that sub-grid variability of snow depth is increasingly compromised by large scale representations of modelled data.

Discussion and Conclusions

By examining the changing snow depth distribution in a subarctic open woodland during a melt season, this study provides an example for systematic comparison of the depth characteristics as represented at three scales (2, 4 and 16 m). The spatial patterns of snow depth reflect the results of the physical melt processes which modify a snow cover initially influenced by the presence of individual stands of spruce trees. The spatial presentation of snow distribution in hydrological models often makes use of grid squares of various dimensions, resulting in varying degrees of generalization and consequent losses of snow information.

The spatial variability of the cell values may be indicated by the standard deviation of snow depth. In an open woodland environment, the seasonal decrease in melt depth is accompanied by an enlargement of the standard deviation but a reduction of the skewness. Local variations of snow depth can be large and this can affect the timing and source areas of meltwater generation. Thus, the loss of local-scale information due to upscaling requires attention.

Upscaling leads to a continual blurring of the spatial details as snow depths are spatially aggregated and some information is lost. The conceptual model given by Eq.(2) is used to examine the loss of information as the size of grid cells increases. Information loss is considered as the absolute value of the difference in depth as presented at two scales. Based on the results from the subarctic woodland site, the loss of information due to upscaling increases as the melt season advances. This is paralleled by a gradual enlargement of the standard deviation.

This study examines only the loss of information due to the upscaling of outputs from a detailed spatial melt model. For modelling on a large scale, input values are subject to upscaling from point or local data, to match the computational grid sizes. The resultant loss of information, when compared with the outputs from models of finer resolution, will necessarily increase. Some of this information pertains to the local level and may not be relevant to the large scale investigations. For the model-

ling of woodland snowmelt, however, sub-grid variability may significantly affect the timing and the source area of meltwater generation and a certain amount of spatial variance needs to be preserved. When applying macro-hydrological models to snowmelt, therefore, it is necessary to ensure that upscaling does not forfeit the information pertinent to the objectives of the studies. Further research along this line will contribute to the topic of scaling in hydrology.

Acknowledgements

This work was funded by a research contract from the Atmospheric Environment Service (now the Meteorological Service of Canada). Field work for this research was supported by a research grant for the Canadian GEWEX provided by the Natural Sciences and Engineering Research Council of Canada. We thank Dr. Barry Goodison for his interest in this project and Professor Lars Bengtsson and other reviewers for their helpful comments.

References

Blöschl, G. (1999) Scaling issues in snow hydrology, *Hydrological Processes, Vol. 13*, pp. 2149-2175.

Blöschl, G., Kirnbauer, R., and Gutknecht, D. (1991a) Distributed snowmelt simulations in an alpine catchment 1. Model evaluation on the basis of snow cover patterns, *Water Resources Research, Vol. 27*, pp. 3171-3179.

Blöschl, G., Kirnbauer, R., and Gutknecht, D. (1991b) Distributed snowmelt simulations in an alpine catchment 2. Parameter study and model predictions, *Water Resources Research, Vol. 27*, pp. 3181-3188.

Buttle, J.M., and McDonnell, J.J. (1987) Modelling the areal depletion of snowcover in a forested catchment, *Journal of Hydrology, Vol. 90*, pp. 43-60.

Cline, D.W., Elder, K., and Bales, R.C. (1998) Scale effects in a distributed snow water equivalence and snowmelt model for mountain basins, *Hydrological Processes, Vol. 12*, pp. 1527-1536.

Davies, J.A., and Idso, S.B. (1979) Estimating the surface radiation balance and its components. In: Barfield, B.J. and Gerber, J.F. (Eds.), *Modification of the Aerial Environment of Plants,* Amer. Soc. Agric. Eng., pp.183-210.

Davis, R.E., Mckenzie, J.C., and Jordan, R.E. (1995) Distributed snow process modeling, Proceedings, 52nd Eastern Snow Conference, Toronto, Canada, pp. 29-38.

Garen, D.C., and Marks, D. (1996) Spatially distributed snow modelling in mountainous regions: Boise River application, in HydroGIS 96: Applications of Geographic Information Systems in Hydrology and Water Resources Management. Proceedings of the Vienna Conference, *IAHS Publication No.* 235, pp. 421-428.

Giesbrecht, M., and Woo, M.K. (2000) Simulation of snowmelt in a subarctic spruce woodland: 2. open woodland model, *Water Resources Research, Vol. 36*, pp. 2287-2295.

Hardy, J.P., Davis, R.E., Jordan, R.E., Ni, W., and Woodcock, C. (1997) Snow ablation modeling in conifer and deciduous stands of the boreal forest, Proceedings, Western Snow Conference, Banff, Canada, pp. 114-124.

Hardy, J.P., Davis, R.E., Jordan, R., Ni, W., and Woodcock, C.E. (1998) Snow ablation modelling in a mature aspen stand of the boreal forest, *Hydrological Processes, Vol.12*, pp.1763-1778.

Hendrie, L.K., and Price, A.G. (1978) Energy balance and snowmelt in a deciduous forest. Proc. on Modeling of Snow Cover Runoff. In: Colbeck, S.C. and Ray, M. (eds.), U.S. Army Cole Regions Research and Engineering Laboratory, Hanover, N.H., pp. 211-221.

Idso, S.B., and Jackson, R.D. (1969) Thermal radiation from the atmosphere, *Journal of Geophysical Reseach, Vol.74(23)*, pp. 5397-5403.

Price, A.G., and Dunne, T. (1976) Energy balance computations of snowmelt in a subarctic area, *Water Resources Research, Vol. 12*, pp. 686-694.

Sturm, M. (1992) Snow distribution and heat flow in the taiga, *Arctic and Alpine Research, Vol. 24*, pp.145-152.

Woo, M.K. (1998) Arctic snow cover information for hydrological investigations at various scales, *Nordic Hydrology, Vol. 29*, pp. 245-266.

Woo, M.K., and Dubreuil, M-A. (1985) Empirical relationship between dust content and Arctic snow albedo, *Cold Regions Science and Technology, Vol.10*, pp.125-132.

Woo, M.K., and Giesbrecht, M. (2000) Simulation of snowmelt in a subarctic spruce woodland: 1. tree model, *Water Resources Research, Vol. 36*, pp. 2275-2285.

Woo, M.K., and Steer, P. (1986) Monte Carlo simulation of snow depth in a forest, *Water Resources Research, Vol. 22*, pp. 864-868.

Received: December, 1999
Revised: 31 August, 2000
Accepted: 1 September, 2000

School of Geography and Geology,
McMaster University,
Hamilton, Ontario,
Canada L8S 4K1.
Email: woo@mcmaster.ca